FIGURE LEGENDS, ONLINE SUPPLEMENT

Figure S1: Western blot analyses for hemagglutinin (HA) - tagged MINT fusion proteins demonstrated expression of all HA-MINT variants. Aliquots of cell lysates were prepared following transient transfection with either empty vector or the indicated CMV-MINT expression constructs. Since all variants possessed the uniform epitope tag for hemagglutinin (HA), the relative expression of each variant and N-terminal fragments could be assessed by Western blot analysis (Arrows, full-length fragments; filled ovals, N-terminal HA-tagged MINT fragments). These analyses demonstrated accumulation of the HA-MINT variants described. Of particular note, full length HA-MINT(1-2400) and HA-MINT(1-2180) proteins accumulated to equivalent levels (Figure S1, lanes 9-12); indeed, MINT(1-2180) accumulates to even slightly higher levels that full length MINT(1-2400) -- and yet MINT(1-2180) does not exhibit capacity to activate OCFRE-dependent transcription as observed with MINT(1-2400) (Figure 1B of the manuscript).

Figure S2: Western blot analyses of cells transfected with EYPF – MINT-NLS eukaryotic expression vectors demonstrated expression of all MINT fusion protein variants. Western blot analysis for the enhanced yellow fluorescence protein (EFYP) tag of the fusion proteins identified expression of all EFYP-MINT variants, with the proline-rich EYFP-MINT-NLS variant migrating more slowly than predicted. Arrows, full length fusion proteins. Asterisk, an EYFP-MINT degradation product.

Figure S3: MINT augments Runx2-dependent transcription in eukaryotic one-hybrid assays. The results obtained using EYFP-MINT(2030-2640)-NLS indicated that OCFRE activation by MINT could be mediated independent of the intrinsic MINT nucleic acid binding activity, but dependent upon Runx2. To provide additional evidence to confirm this notion, we implemented the one hybrid assay of FGF2-regulated Runx2 TAF (transactivation function). In this assay, transcriptional regulation is driven by Runx2 TAF present in chimeric Gal4 DNA binding domain (G4) – Runx2 fusion protein (see Figure 2 of the manuscript); however, the TAF is recruited to a heterologous pFR-LUC via the G4 DNA recognition cognate multimerized upstream of the reporter transcription initiation site. As shown, full length MINT(1-3576) augmented transcription driven by G4-Runx2 in FGF2-treated cultures. MINT(1141-3576) also significantly activated FGF2-stimulated G4-Runx2 transcription. Thus, as observed in OCFRE activation, activation of Runx2 TAF in one-hybrid analysis did not require the N-terminal RRM domains of MINT. All transcription was dependent upon Runx2 recruitment via the Gal4DBD to the Gal4 cognates of pFR-LUC, since expression of Runx2 without the G4 fusion failed to mediate any significant activity.

Figure S4: Western blot analyses of cells transfected with pcDNA3-Runx2 variant eukaryotic expression vectors demonstrated equivalent expression of wild type Runx2, Runx2(S301A,S319A,T326A), and Runx2(S301D,S319D,T326D) variants. Western blot analyses indicate that the protein accumulation of Runx2, Runx2(S301A, S319A, S326A), and Runx2(S301D, S319D, S326D) are routinely equivalent following transient transfection. Activation by MINT is significantly decreased in the Runx2(S301A,S319A,T326A) variant lacking intact proline-directed protein kinase (PKPD) motifs in Runx2 activation domain 3 (AD3; see Figure 4F manuscript). Activation by MINT is significantly increased in the Runx2(S301D, S319D, S326D) "phosphomimetic" variant (Figure 4F, manuscript).

Figure S5: Activation of Runx2 by MINT+FGF2 is inhibited by DMAT, but not more selective CK2 kinase antagonists. MINT+FGF2 activation of the OCFRE7-RSVLUC reporter was assessed in transient transfection assays in the presence or absence of specific protein kinase inhibitors. DMAT, an inhibitor of both Dyrk/HIPK and CK2 kinases, significantly reduced MINT+FGF2 activation of the OCFRE. However, selective CK2 inhibitors such as emodin and ellagic acid did not inhibit activation by MINT+FGF2.

Figure S6: HIPK3-directed siRNA decreases EGFP-HIPK3 protein accumulation in transiently transfected cells. Cells were co-transfected with either control scrambled siRNA or anti-HIPK3 siRNA and a CMV eukaryotic expression construct for an EGFP (enhanced green fluorescence protein) – HIPK3 protein. Cultures were evaluated for expression of the EGFP-HIPK3 fusion using epifluorescent illumination and digital photomicrography to score the number of cells positive for signal. Upper panels, phase contrast view. Lower panels, epifluorescence image. HIPK3 siRNA significantly reduced expression of EGFP-HIPK3 fusion protein ($p < 0.0001$; Chi-squared Fisher's exact test).

Figure S7: HIPK3 Binds to Runx2. In vitro synthesized and unlabeled Runx2 co-immunoprecipitates radiolabeled HIPK3 (lanes 2, 5-6), but not radiolabeled OPN (lanes 1, 3-4).

Figure S8: DMAT inhibits FGF2-stimulated Runx2 protein accumulation. C3H10T1/2 cells were transiently transfected with the pcDNA3-Runx2 expression construct, and treated with FGF2 either in the presence or absence of 20 uM DMAT. Note that while FGF2 stimulates Runx2 protein abundance, while co-treatment with DMAT abrogates FGF2 actions.

Figure S9. Working model of OCFRE regulation by MINT. FGF2 upregulates activity via a multiprotein nuclear complex assembled by the OCFRE, contacting Ku antigen and Runx2 (1-3), Transactivation function (TAF) resides in Runx2(2), and Runx2 AD3 is increased by MINT+FGF2. MINT activation requires the MID domain, a target of Msx2-dependent inhibition of the OCFRE(2, 4). Although the MINT RRM domain binds the OCFRE and significantly promotes transactivation, core activation function maps to the MID domain. FGF2/FGFR activation requires HIPK3, a proline-directed kinase that phosphorylates Runx2, controls Runx2 protein accumulation, binds both Runx2 and MINT MID domain, co-localizes with MINT in the nucleus, and supports *OC* gene expression. OSE2, osteoblast specific element- 2 (5).

REFERENCES CITED, ONLINE SUPPLEMENT

1. **Willis DM, Loewy AP, Charlton-Kachigian N, Shao JS, Ornitz DM, Towler DA** 2002 Regulation of osteocalcin gene expression by a novel Ku antigen transcription factor complex. J Biol Chem 277:37280-91
2. **Sierra OL, Cheng SL, Loewy AP, Charlton-Kachigian N, Towler DA** 2004 MINT, the Msx2 interacting nuclear matrix target, enhances Runx2-dependent activation of the osteocalcin fibroblast growth factor response element. J Biol Chem 279:32913-23
3. **Newberry EP, Boudreaux JM, Towler DA** 1997 Stimulus-selective inhibition of rat osteocalcin promoter induction and protein-DNA interactions by the homeodomain repressor Msx2. J Biol Chem 272:29607-13
4. **Newberry EP, Latifi T, Battaile JT, Towler DA** 1997 Structure-function analysis of Msx2-mediated transcriptional suppression. Biochemistry 36:10451-62
5. **Ducy P, Zhang R, Geoffroy V, Ridall AL, Karsenty G** 1997 Osf2/Cbfa1: a transcriptional activator of osteoblast differentiation. Cell 89:747-54

Figure S1

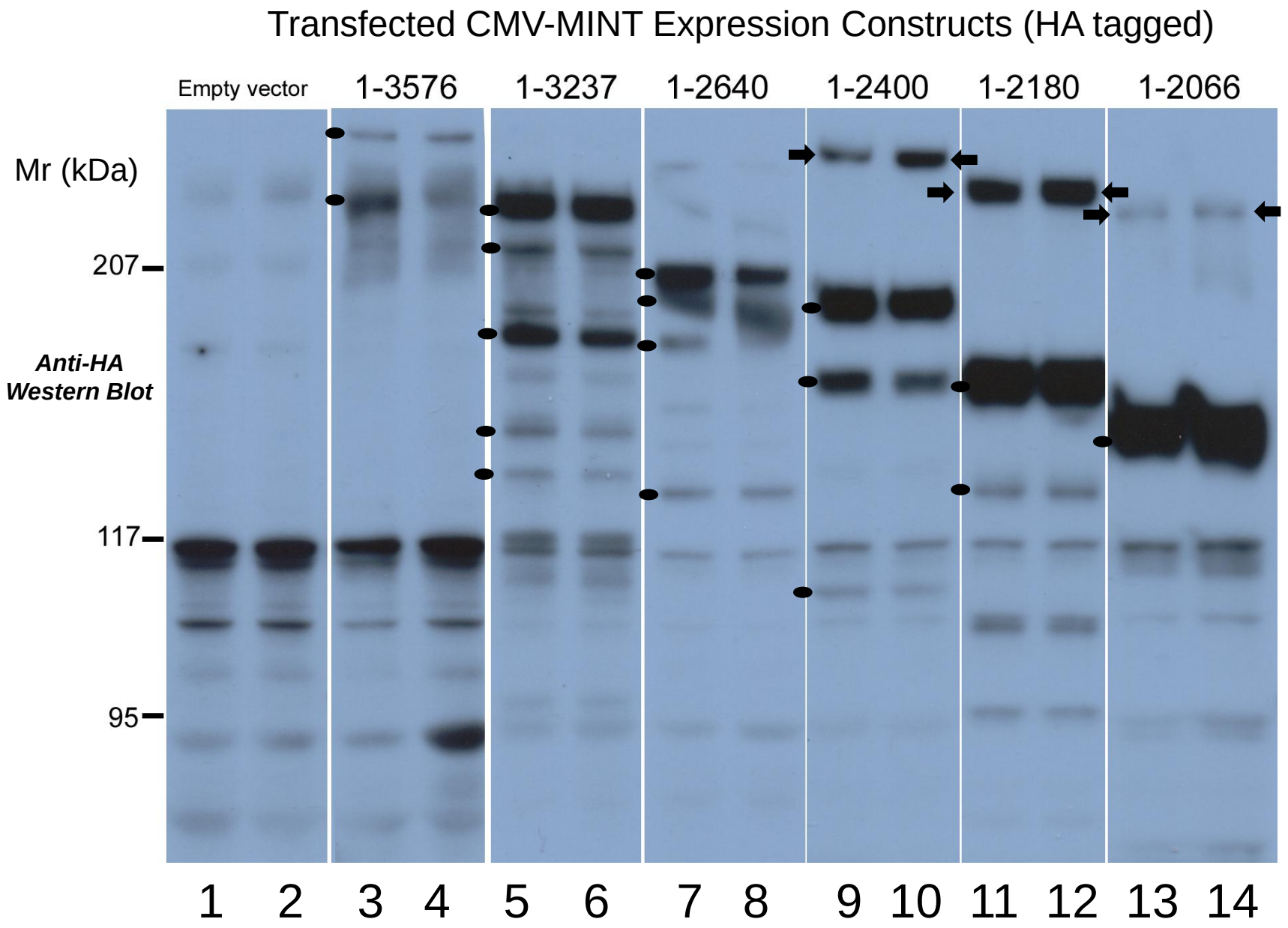
Transfected CMV-MINT Expression Constructs (HA tagged)
Empty vector
1-3576
1-3237
1-2640
1-2400
1-2180
1-2066
Mr (kDa)
207
117
95
Anti-HA
Western Blot
1 2 3 4 5 6 7 8 9 10 11 12 13 14

Figure S2

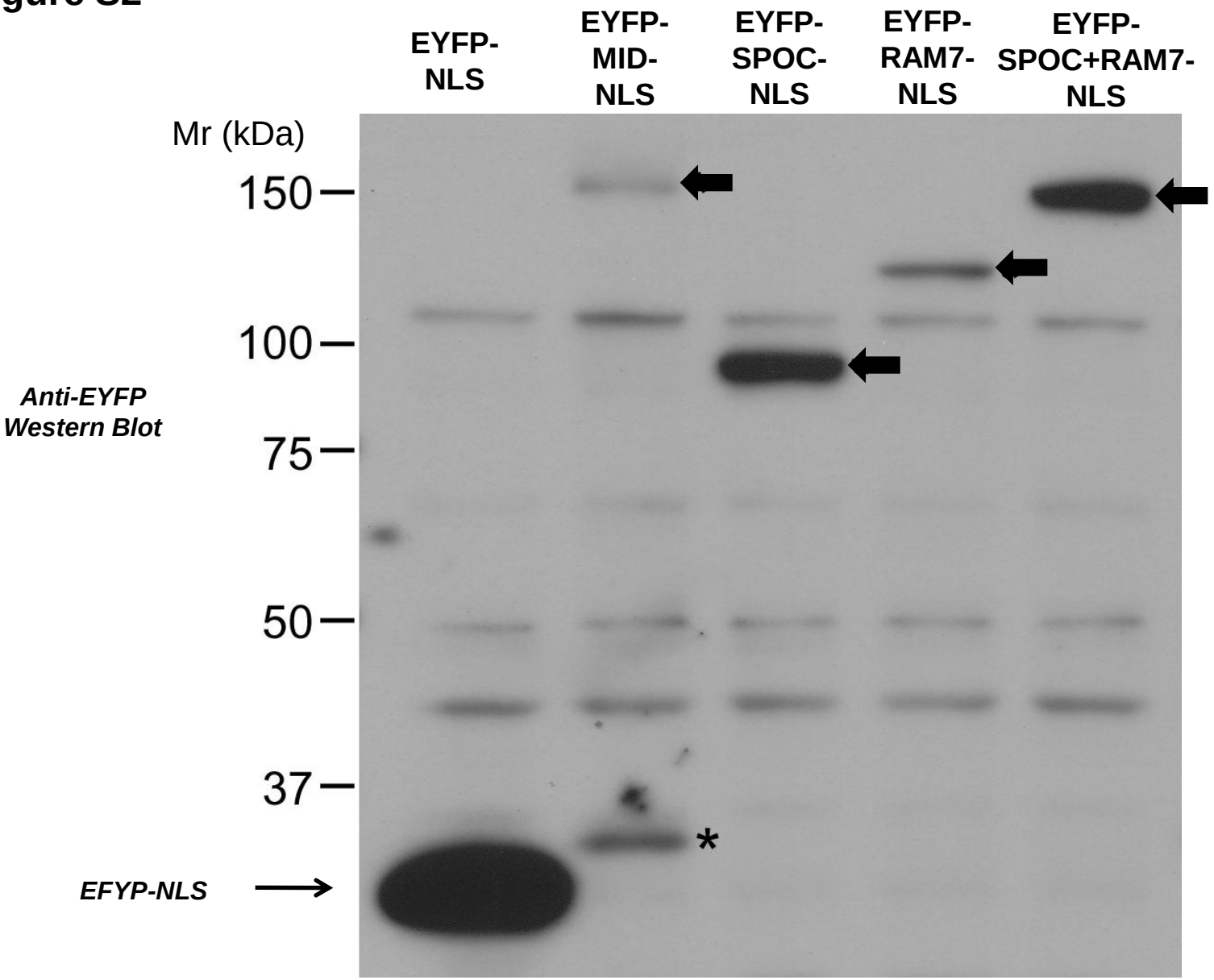
EYFP-NLS
EYFP-MID-NLS
EYFP-SPOC-NLS
EYFP-RAM7-NLS
EYFP-SPOC+RAM7-NLS
Mr (kDa)
150
100
75
50
37
Anti-EYFP Western Blot
EFYP-NLS
*

Figure S3

ANOVA p < 0.0001

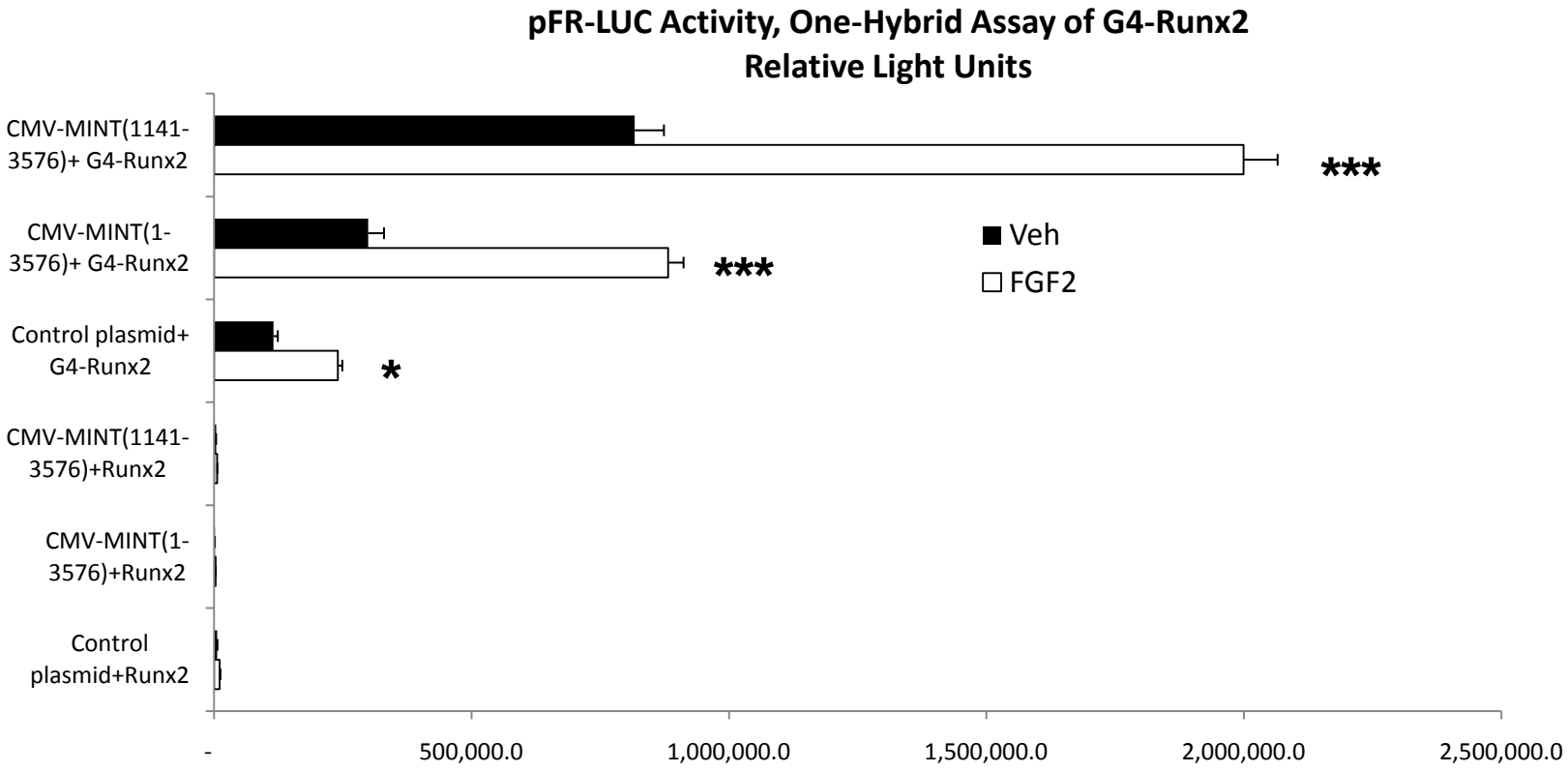

Figure S4

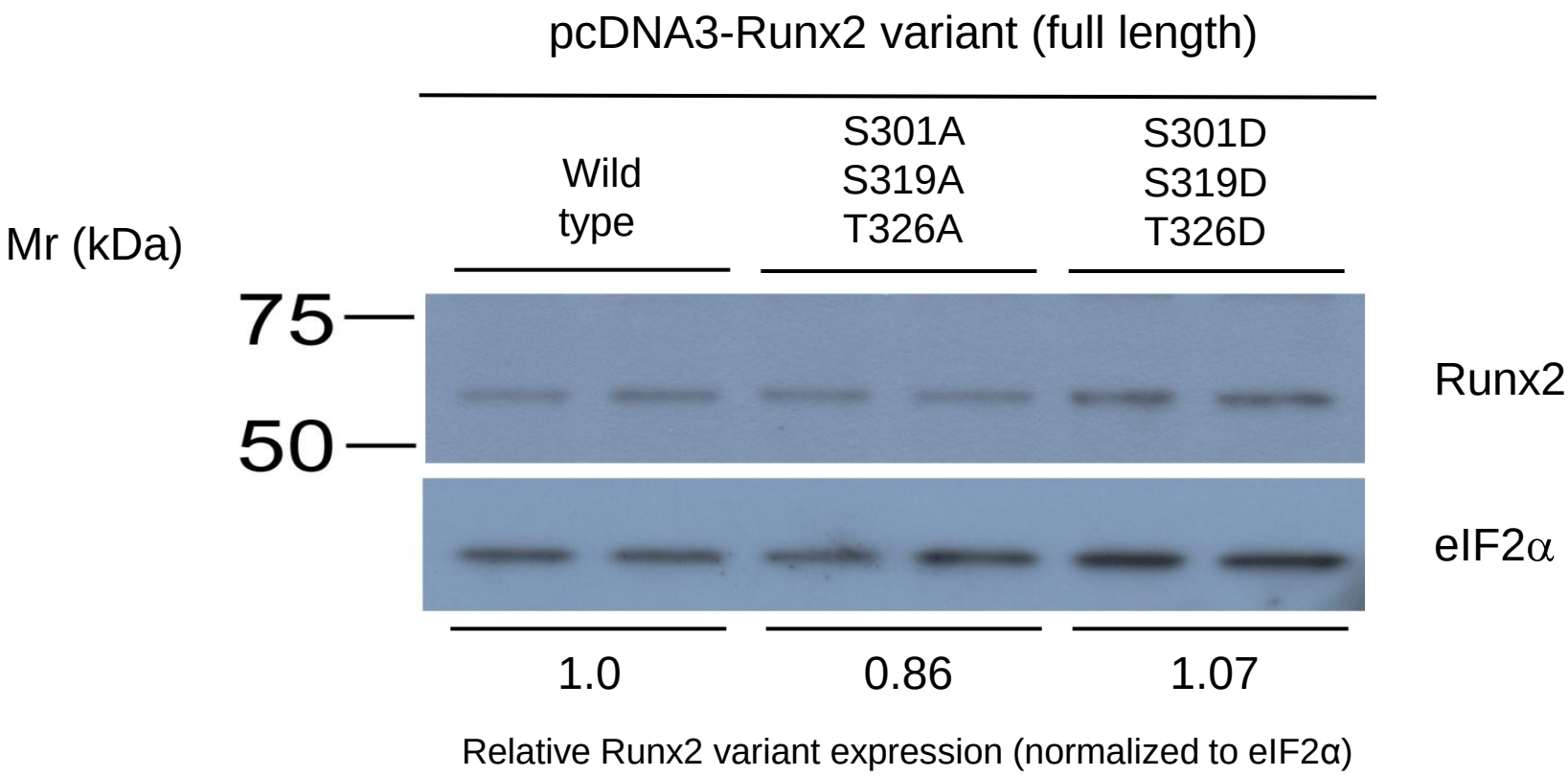

Relative Runx2 variant expression (normalized to eIF2α)

Figure S5

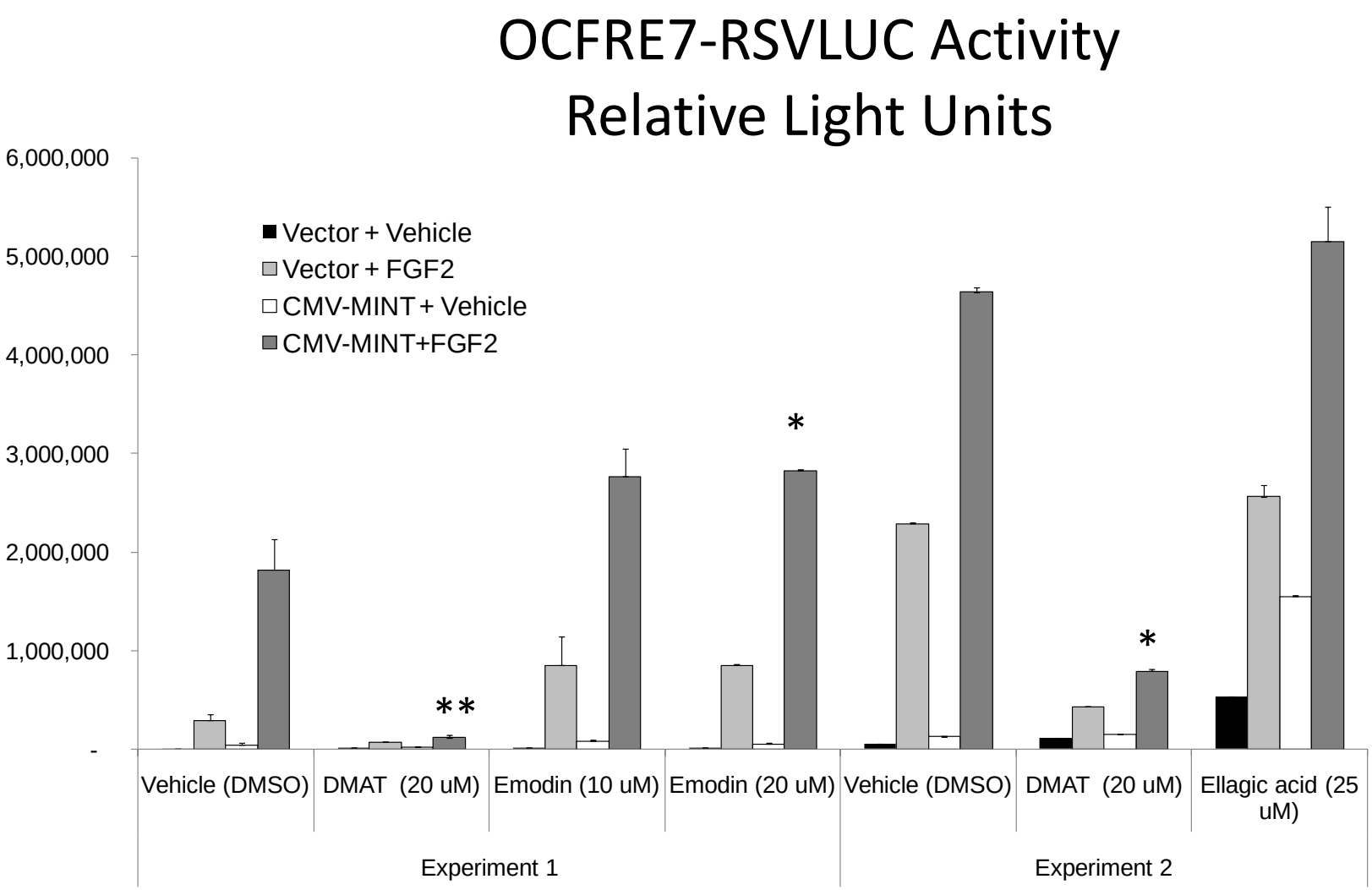

ANOVA p = 0.0017

Figure S6

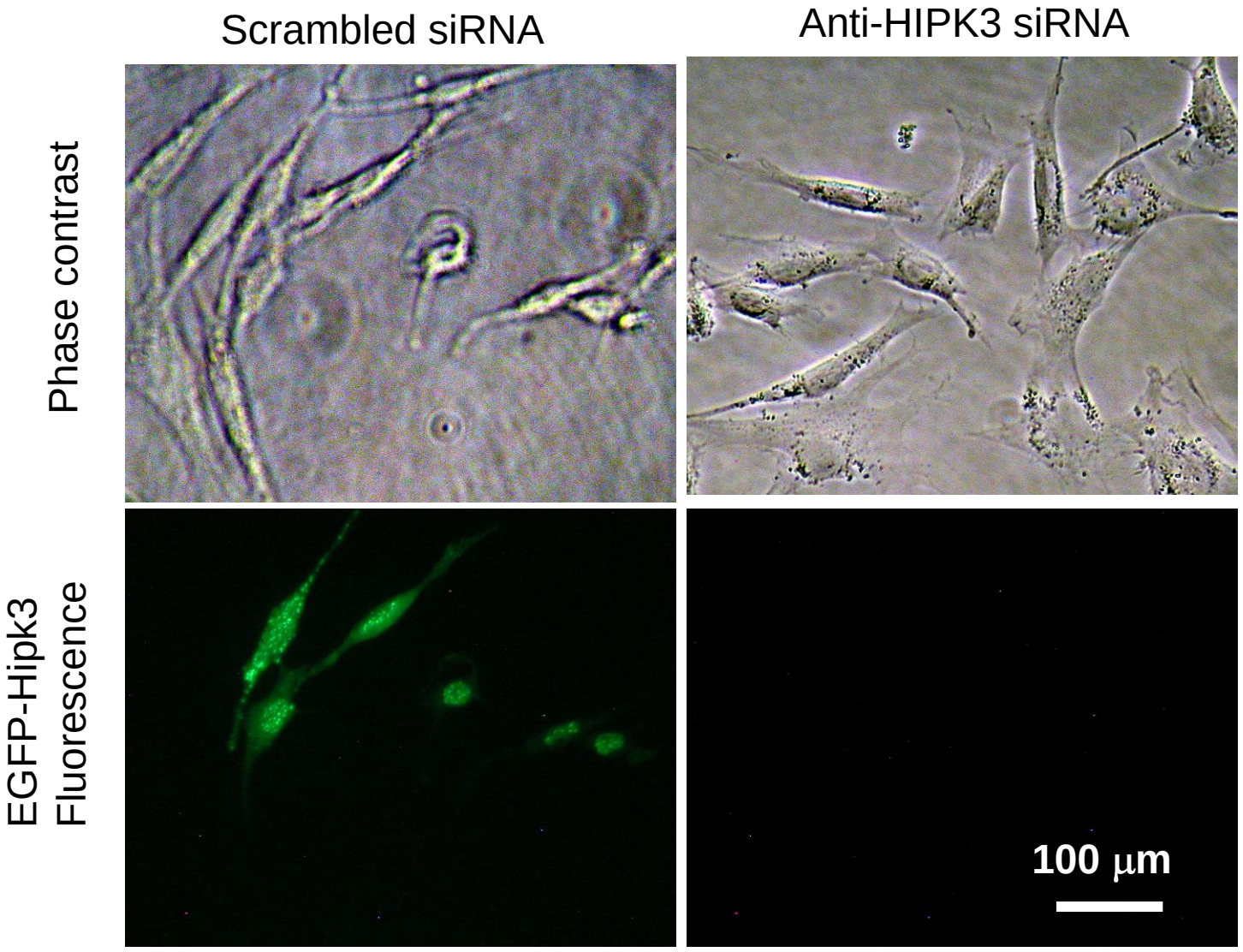

$p < 0.0001$
χ^2 Fisher's Exact Test

Figure S7

HIPK3 Binds Runx2

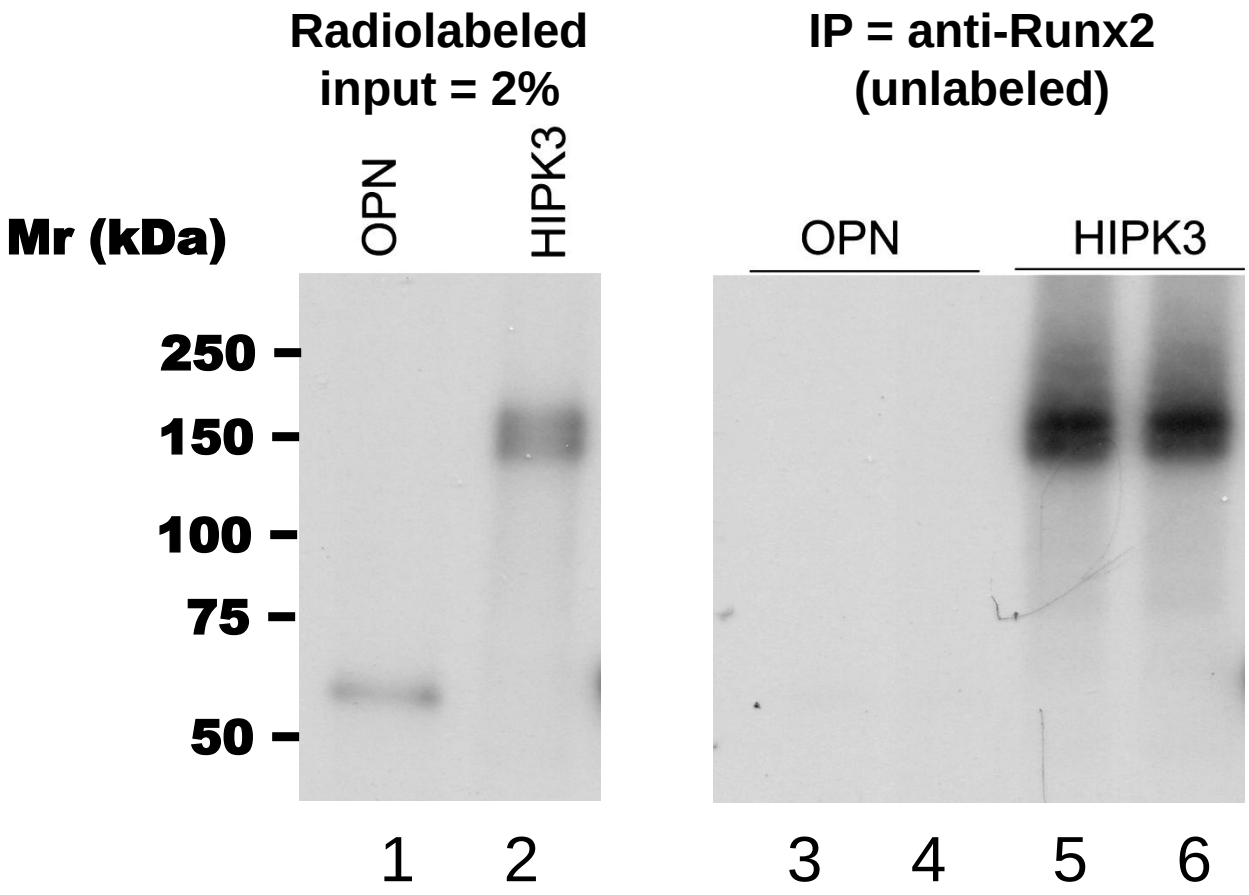

Figure S8

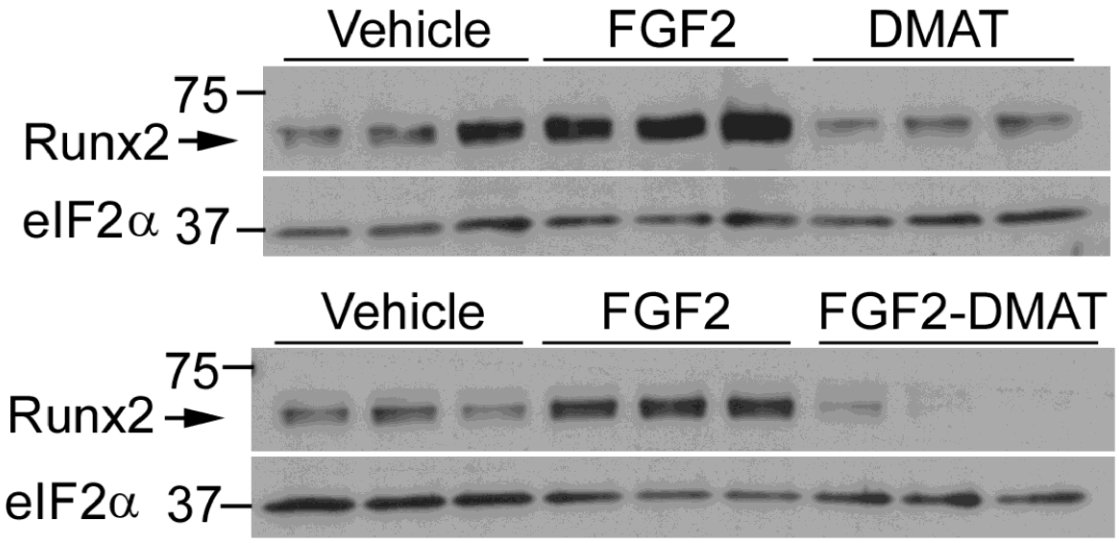
Vehicle
FGF2
DMAT
75
Runx2
eIF2α 37
Vehicle
FGF2
FGF2-DMAT
75
Runx2
eIF2α 37

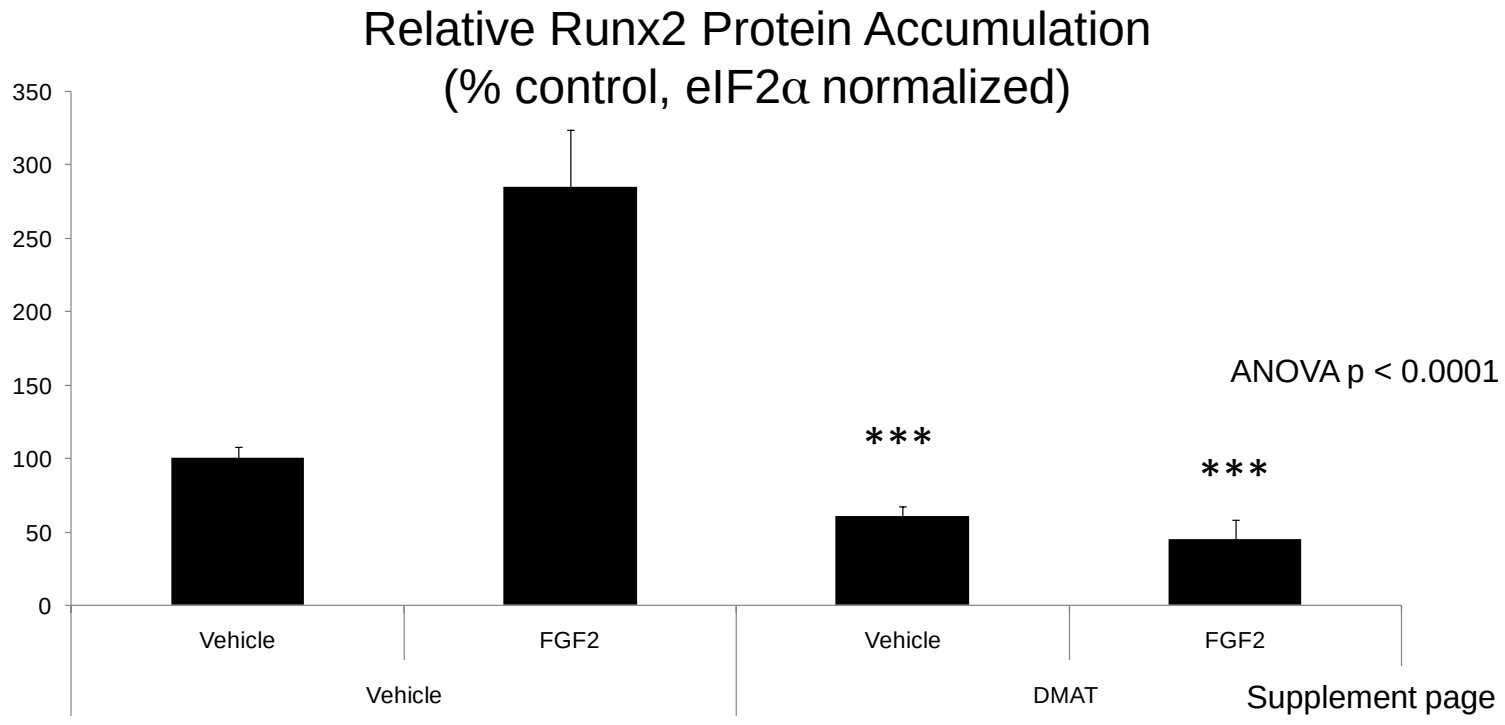
Relative Runx2 Protein Accumulation
(% control, eIF2α normalized)
350
300
250
200
150
100
50
0
***
***
ANOVA p < 0.0001
Vehicle
FGF2
Vehicle
FGF2
Vehicle
DMAT

Figure S9

Working Model of OCFRE Regulation